Journal of Magnetic Resonance 195 (2008) 162–168

Contents lists available at ScienceDirect

Journal of Magnetic Resonance

journal homepage: www.elsevier.com/locate/jmr

A dynamic nuclear polarization strategy for multi-dimensional Earth's field NMR spectroscopy

Meghan E. Halse, Paul T. Callaghan *

MacDiarmid Institute for Advanced Materials and Nanotechnology, School of Chemical and Physical Sciences, Victoria University of Wellington, Post Office Box 600, Wellington 6012, New Zealand

ARTICLE INFO

Article history:
Received 2 August 2008
Revised 5 September 2008
Available online 17 September 2008

Keywords:
Earth's magnetic field
Dynamic nuclear polarization
Sensitivity enhancement
Multi-dimensional spectroscopy
Nuclear magnetic resonance

ABSTRACT

Dynamic nuclear polarization (DNP) is introduced as a powerful tool for polarization enhancement in multi-dimensional Earth's field NMR spectroscopy. Maximum polarization enhancements, relative to thermal equilibrium in the Earth's magnetic field, are calculated theoretically and compared to the more traditional prepolarization approach for NMR sensitivity enhancement at ultra-low fields. Signal enhancement factors on the order of 3000 are demonstrated experimentally using DNP with a nitroxide free radical, TEMPO, which contains an unpaired electron which is strongly coupled to a neighboring ^{14}N nucleus via the hyperfine interaction. A high-quality 2D ^{19}F–^{1}H COSY spectrum acquired in the Earth's magnetic field with DNP enhancement is presented and compared to simulation.

1. Introduction

Earth's field nuclear magnetic resonance (EFNMR), which is nearly as old as NMR itself [1,2], has long been used in the field of magnetometry and for teaching the principles of magnetic resonance to students. More recently, however, EFNMR has been shown to have promise for a much broader range of applications including multi-dimensional imaging [3–5], high-resolution spectroscopy [6–9] and measurements of molecular diffusion [10–13].

While EFNMR enjoys the advantage of sub-hertz spectral resolution over large (>100 mL) sample volumes due to the natural homogeneity of the Earth's field, it suffers from low sensitivity, a consequence of the approximate B_0^2 dependence of signal-to-noise ratio (SNR) on field strength, which for the Earth's field is on the order of 50 μT (0.5 G). In addition, at the Larmor frequency of protons in the Earth's field (~2 kHz), the observed noise is dominated by external interference not by the Johnson noise of the detection coil. In order to fully realise the potential of Earth's field NMR, clever strategies for sensitivity enhancement need to be employed. The ultimate goal of the work presented herein is the acquisition of high quality, multi-dimensional NMR spectra in the Earth's magnetic field. Therefore, a strong emphasis is placed on sensitivity enhancement methods which are readily adapted to multi-dimensional experiments.

A relatively obvious solution to the problem of external noise interference involves the use of Faraday screening to reduce ultra-low frequency (ULF) noise pickup. Alternatively, the observed SNR of the EFNMR signal can be enhanced through the use of novel non-Faraday induction detection schemes such as atomic magnetometers [14] or super-conducting quantum interference devices (SQUIDs) [15]. This paper, however, will be concerned exclusively with the sensitivity enhancement which can be achieved within the realm of Faraday induction.

The problem of overcoming the very low thermal polarization available at 50 μT can be addressed using one of two general strategies. The first is prepolarization [1], whereby the sample is allowed to come to thermal equilibrium in a strong, but not necessarily homogeneous, magnetic field prior to excitation and detection in the highly homogeneous Earth's magnetic field. The second is hyperpolarization, whereby the polarization of the target nuclear spin is enhanced beyond thermal equilibrium polarization by means of a polarization transfer from a second group of spins with a much higher level of polarization. An example of this is dynamic nuclear polarization (DNP) where the polarization transfer occurs between unpaired electron spins and the target nuclear spins via the so-called Overhauser effect [16]. DNP has been very successfully implemented in conjunction with Earth's field magnetometers both for raw signal enhancement and for a clever noise cancellation scheme [17].

2. Theory

2.1. Prepolarization

Conceptually, one of the simplest approaches to sensitivity enhancement is to prepolarize the sample using a strong but not necessarily homogeneous magnetic field prior to excitation and detection in a weaker but highly homogeneous magnetic field.

* Corresponding author. Fax: +64 4 463 5237.
E-mail address: Paul.Callaghan@vuw.ac.nz (P.T. Callaghan).

1090-7807/$ - see front matter © 2008 Elsevier Inc. All rights reserved.
doi:10.1016/j.jmr.2008.09.007

In the 2D COSY pulse sequence presented in Fig. 1, the sample is exposed to the polarizing field, B_{polz}, for a period, t_{polz}, during which it comes to either full or partial thermal equilibrium with this field. This polarization field is then removed from the sample and following a delay, t_d, the enhanced polarization is excited and detected in the highly homogeneous Earth's magnetic field, B_E. The maximum achievable enhancement factor (EF) relative to thermal polarization in the Earth's field is given by Eq. (1). Note that this expression assumes that the sample is allowed to come to full thermal equilibrium in the polarization field, i.e. $t_{polz} \geqslant 5T_1$

$$\mathrm{EF} = \frac{B_{polz}}{B_E} e^{-\frac{t_d}{T_1}}. \quad (1)$$

Eq. (1) indicates that in order to achieve significant enhancements the polarization field must be large relative to the Earth's field and the delay time, t_d, between the polarization phase and the detection phase of the pulse sequence must be very short compared to T_1. In the context of multi-dimensional spectroscopy, it is very important that the enhancement factor is constant between successive transients. Therefore, it is imperative that the polarizing field strength, B_{polz}, the polarizing time, t_{polz}, and the polarization to detection delay, t_d, are constant.

In any prepolarization scheme, the polarization field can be generated by either an electromagnet or a permanent magnet array. First consider the case of an electromagnet, which is very advantageous for a variety of reasons. First, it is relatively easy and cost effective to construct an electromagnet which is not particularly homogeneous, that is with a homogeneity on the order of a few percent rather than a few parts per million (ppm). Second, the field of the electromagnet can be switched on and off as required, providing the user with sufficient control over B_{polz}, t_{polz} and t_d to ensure a constant enhancement factor between transients. Third, the field is under software/spectrometer control and therefore is easily used in multi-dimensional experiments. There are, however, several practical limitations. The first concern is field strength. In order to achieve large magnetic fields with an electromagnet, large currents must be used and this can result in significant resistive heating in the coil. Coil heating can be dealt with through the use of water cooling but this greatly complicates the overall system and limits its size, cost and portability. The second concern, which is also a matter of resistive heating, is the polarization time. Long T_1 samples will require long polarization times which will enhance the problem of coil heating. The final practical concern is associated with the rapid switching of a strong polarizing field. If Faraday screening is employed to reduce pick-up of external ULF noise, rapid switching of a strong polarizing field will give rise to strong eddy currents in the screen and so the delay time, t_d, will need to be sufficiently long so that there are no time dependent disruptions to the homogeneity of the Earth's field during detection.

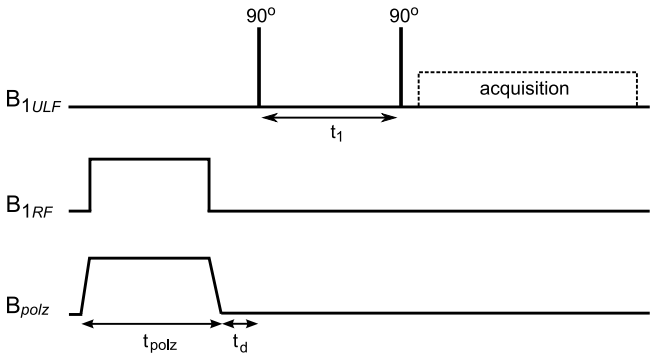

Fig. 1. Pulse sequence diagram for a 2D correlation spectroscopy (COSY) experiment with prepolarization (B_{polz}) and/or DNP irradiation (B_{1RF}) prior to signal excitation and detection in the Earth's magnetic field (B_{1ULF}). For multi-dimensional spectroscopy experiments, consistency of timing in the prepolarization phase and the delay time, t_d, is essential.

As shown by Appelt et al. [7], an attractive solution for single-shot experiments is the use of a permanent magnet Halbach array for prepolarization. If high homogeneity is not a concern, Halbach arrays with field strengths of up to 1 T can be constructed without much difficulty. One of the significant advantages of the Halbach design is that these arrays are largely self-screening and so can be located within a few meters of the Earth's field NMR probe without significantly disrupting the homogeneity of the detection field. If shimming is available, the Halbach array can be located as close as 1–1.5 m from the EFNMR probe without disrupting the sub-hertz spectral resolution. In addition, all of the electromagnet concerns of resistive heating and field switching are removed with the use of a Halbach array. The most significant disadvantage of the Halbach prepolarization approach lies in the transfer of the sample from the Halbach array to the EFNMR probe. In [7] this transfer was done manually and transfer times were on the order of seconds. In a multi-dimensional experiment, sample transport from Halbach to EFNMR probe would be very challenging to automate, especially in terms of maintaining a constant polarization time and transfer time. Therefore, this is not an attractive solution for the purposes of multi-dimensional spectroscopy.

2.2. Dynamic nuclear polarization

DNP is a technique for enhancing, above its thermal equilibrium value, the polarization of a target nuclear spin, a proton for example, by means of a net polarization transfer from an excited unpaired electron spin via the process of cross-relaxation. This polarization transfer is commonly achieved in liquids by means of the Overhauser effect. In most applications where DNP is used for signal enhancement, the free electron must be introduced into the sample via the addition of a free radical. The most commonly used DNP free radicals are nitroxide radicals, such as 2,2,6,6-tetramethylpiperidine 1-oxyl (TEMPO).

The DNP process can conceptually be divided into two phases: (1) the excitation of the electron spins and (2) the polarization transfer between the excited electron spins and the target nuclear spins. The excitation of the electron spins, phase 1, can only be achieved and optimized through a thorough theoretical understanding of the energy levels and transition probabilities of the free electron spin system. The transfer of polarization between the electron spins and the target nuclear spins, phase 2, can be understood and quantified through a consideration of the so-called Solomon equations [18].

For the purposes of this discussion of DNP in the Earth's magnetic field, the TEMPO free radical containing ^{14}N at natural abundance (99.6%) will be considered, exclusively. Therefore, in terms of determining the allowed transitions of the electron spins, the system under consideration contains a single free-electron spin, with a spin quantum number $s = 1/2$, and a single ^{14}N nuclear spin, with a spin quantum number $k = 1$. There exist a number of ^{1}H spins within the free radical molecule; however, these nuclear spins are far removed from the site of the free-electron. For the purposes of this discussion, any intramolecular hyperfine coupling between the free electron and these ^{1}H nuclear spins will be considered to be negligible.

For a given solvent-dependent hyperfine coupling constant, A, between the electron spin, S, and the nuclear spin, K, and in the presence of an external magnetic field $\mathbf{B_0} = B_0\hat{z}$ the spin Hamiltonian can be written, in angular frequency units, as follows:

$$\mathscr{H} = -\gamma_S B_0 \mathbf{S_z} - \gamma_K B_0 \mathbf{K_z} + A\mathbf{S}\cdot\mathbf{K}. \quad (2)$$

This Hamiltonian is not diagonal in either of the product operator or the total angular momentum representations. In the high field case, where $\gamma_S B_0 \gg A$, the product operator formalism, characterised by the azimuthal spin quantum numbers m_S and m_K, is typically used and the hyperfine coupling term is treated as a perturbation to the dominant Zeeman terms. However, in ultra-low fields such as the Earth's magnetic field (~50 μT) the hyperfine coupling term is strongly dominant. Therefore, this system needs to be solved exactly in order to understand the system under the influence of magnetic fields ranging from the Earth's field to the mT fields used for prepolarization. A detailed quantum mechanical description of this system can be found in [19].

The six energy levels of the coupled spin system, given by the Breit Rabi equations [20], are shown in Fig. 2 as a function of field, B_0. This plot clearly indicates the transition from the ultra-low field case where the hyperfine coupling term is dominant to the "high" field case where the electron Zeeman term is dominant. In the ultra-low field case, the signal enhancement is potentially orders of magnitude larger than the theoretical maximum DNP enhancement in the high field case (~658 for protons). This is a consequence of the fact that the hyperfine field of the ^{14}N nucleus experienced by the unpaired electron is much larger than the prevailing static magnetic field and therefore the polarization of the electron spin is much higher than the thermal polarization predicted by the Zeeman interaction alone.

There are 10 allowed transitions for this two-spin system. These include eight π transitions, which can be induced by a B_{1RF} applied perpendicular to B_0 and two σ transitions, which can be induced by a B_{1RF} applied parallel to B_0. Fig. 3 presents a plot of the frequencies of these allowed transitions as a function of field, B_0. The six transitions which are of interest over the range of fields shown are labeled in Fig. 3. Of these, T_{26} and T_{35} are σ transitions while the others are π transitions. A calculation of transition probabilities [19] shows that the σ transitions can only be induced at very low B_0 values whereas all of the π transitions, with the exception of T_{45}, have significant transition probabilities over the range of fields shown. The transition probability of T_{45} drops off significantly with increasing B_0 in a manner analogous to the decrease in transition frequency.

In order to achieve a polarization transfer between the unpaired electron spins and the target nuclear spins of the solvent, one or more of these transitions needs to be excited. This is achieved through the application of a continuous wave (CW) radiofrequency (RF) field, B_{1RF}, at a particular transition frequency. There are two approaches to selecting the transition and field strength at which this is achieved.

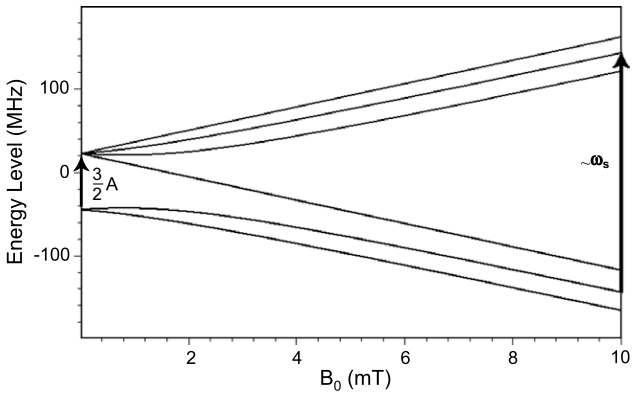

Fig. 2. Energy level frequencies as a function of static field strength, B_0, for the coupled two spin, electron and ^{14}N nucleus, system in 2,2,6,6-tetramethylpiperidine 1-oxyl (TEMPO). At ultra-low fields the hyperfine coupling between the electron and the nitrogen nucleus dominates whereas at higher fields (10 mT) the electron Larmor term dominates. $2\pi * 45$ MHz was used for A in this calculation.

The first and most straightforward approach is to apply the RF excitation in the presence of only the Earth's magnetic field, B_E. This approach has been previously reported for sensitivity enhancement of Earth's field magnetometers [17,21] and for Earth's field NMR imaging [22]. As indicated by the vertical line in Fig. 3, this corresponds to a transition frequency (for T_{16}) of approximately 68 MHz. Since the field value is fixed as $B_0 = B_E$, determining the exact transition frequency in practice requires successive re-tuning and matching of the B_{1RF} coil over a range of frequencies. The exact resonant frequency of the transition is then deduced as that corresponding to the largest observed signal enhancement. This process can be time consuming and is not easily automated; however, it does have the advantage of requiring no other external magnetic field than the Earth's field itself.

In the second approach, following the field-cycled DNP experiment previously reported for indirect observation of electron paramagnetic resonance (EPR) spectra via DNP [19,22–26], a higher frequency is chosen, for example 131.5 MHz, at which the B_{1RF} coil tunes and matches very well. A CW RF field at this frequency is applied in the presence of a weak prepolarizing field generated by an electromagnet (as in Fig. 1). Note that this prepolarizing field will necessarily be stronger than the Earth's magnetic field, but it can be far below the value where some of the heating and eddy current problems of large electromagnetic prepolarization fields are experienced. In order to determine the field at which a maximum enhancement is achieved, the strength of the prepolarizing field is iteratively varied, in the manner of field-cycled NMR, and the resultant signal is observed. The DNP enhancement will increase and decrease as the chosen irradiation frequency moves in and out of resonance with the various electron transitions. This is illustrated by the data in the inset of Fig. 3. It is clear from this data that for TEMPO in aqueous solution a maximum enhancement for an irradiation frequency of 131.5 MHz is achieved in a field of 2.7 mT. This corresponds to the T_{16} transition. The benefit of this field cycled approach for opimizing the DNP signal enhancement is not only larger signal enhancements compared to DNP performed directly in the Earth's magnetic field due to the higher irradiation frequency but also a simplification and potential automation of the signal enhancement optimization.

Given the excitation of a specific transition, the resultant polarization transfer from the excited electron spins, S, to the target nuclear spins, I, can be described and quantified using the Solomon equation [18], which defines the maximum DNP factor, DNPF, in terms of the ratio of the polarization of the excited electron spins to the thermal equilibrium polarization of the nuclear spins, I_0, scaled by f, the leakage factor, s, the saturation factor and ρ, the coupling factor. S_0 is the thermal polarization of the electron spins and $\langle S_z \rangle$ is the ensemble average expectation value of the electron polarization under the influence of the cw DNP irradiation

$$\mathrm{DNPF} = \frac{\langle I_z \rangle - I_0}{I_0} = -\rho f s \left(\frac{\langle S_z \rangle - S_0}{I_0} \right). \tag{3}$$

The coupling factor, ρ, is a measure of the efficiency of the coupling between the electron spin and the nuclear spin and is a function of the dominant coupling mechanism. Theoretically, ρ has a value of -1 for pure scalar interactions and has a value of 0.5 for pure dipolar coupling [19]. In this work, liquid systems with relatively low free radical concentrations are used and therefore it is assumed that the dominant coupling mechanism between the target nuclear spins and the unpaired electron spins is the dipolar interaction.

The leakage factor is a measure of how much of the spin-lattice relaxation of the target nuclei is driven by interactions with the

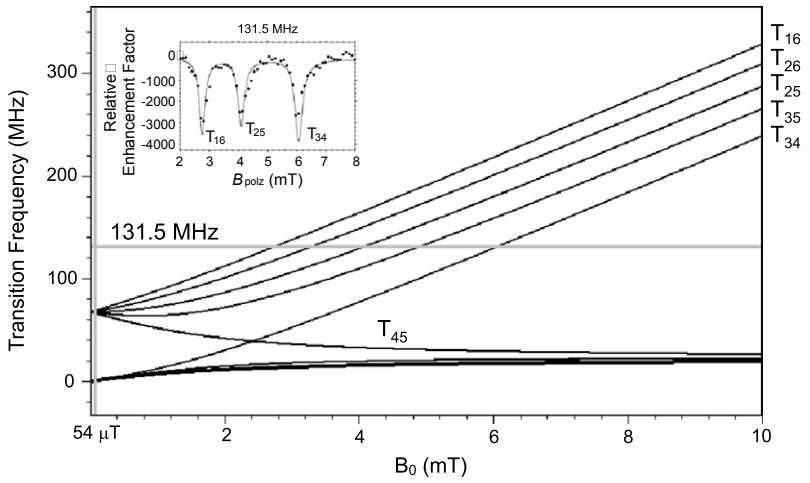

Fig. 3. Transition frequencies as a function of B_0 for the 10 allowed transitions of the unpaired electron coupled to a ^{14}N nucleus in a TEMPO molecule ($A = 2\pi * 45$ MHz). The transitions with appreciable frequencies over the range of fields shown are labeled. T_{16}, T_{45}, T_{34} and T_{25} are π transitions. T_{26} and T_{35} are σ transitions. The σ transitions have significant transition probabilities only at ultra-low B_0 values and so cannot be easily excited at higher values of B_0. The vertical gray line indicates the position of the Earth's field at ~54 μT, while the fields at which 131.5 MHz transitions occur are indicated by the horizontal gray line. Inset is an experimental measurement of the observed signal enhancement, relative to thermal polarization in the Earth's field (54 μT), with a DNP irradiation applied at 131.5 MHz in the presence of a range of prepolarization fields from 2 mT to 8 mT. It is clear that the maximum signal enhancement is observed at 2.7 mT, which corresponds to the T_{16} transition. The sample was a 1.5 mT aqueous solution of TEMPO. B_{1RF} was oriented perpendicular to B_p and therefore only π transitions are observed.

electron spins. The leakage factor, f, can be calculated using the following equation:

$$f = 1 - \frac{T_1}{T_{1,0}}, \tag{4}$$

where $T_{1,0}$ is the spin-lattice relaxation time of the nuclear spin ensemble in the absence of the free radical and T_1 is the spin-lattice relaxation time in the presence of the free radical. Clearly Eq. (4) presents us with the need for a compromise. A value of f close to the maximum of unity implies a significantly faster free-radical induced relaxation and hence a broadening of the proton homogeneous linewidth.

The saturation factor is a measure of the saturation of the chosen transition and is a function of RF power and the properties of the RF resonator. A more comprehensive discussion of the saturation factor, the coupling factor and the leakage factor in the context of DNP at high magnetic fields can be found in [27].

In order to determine the maximum DNP factor for the various transitions as a function of B_0, the expectation value of the electron spin system is evaluated assuming total saturation of the transition, i.e. assuming the equalization of the populations of the two energy levels involved in the chosen transition. For the calculation of the maximum DNP factors, the saturation and leakage factors are assumed to be 1 and the coupling factor is assumed to be 0.5, the theoretical maximum for a liquid system where cross-relaxation is dominated by dipole coupling. Enhancement factors are calculated relative to the thermal equilibrium polarization of protons in an Earth's magnetic field of 54 μT.

Fig. 4 presents the relative enhancement factors of four π transitions, T_{16}, T_{45}, T_{25} and T_{34}, and two σ transitions, T_{26} and T_{35}, over a range of prepolarization fields from 54 μT (no prepolarization) to 10 mT (moderate prepolarization). For comparison, the maximum enhancement factor achievable by a prepolarizing field of 1 T (without DNP) is indicated by the dotted line. This plot illustrates the dramatic sensitivity enhancements which are possible using DNP. This enhancement is much larger than the high field maximum DNP enhancement given by the ratio of gyromagnetic ratios (~658 for protons) because of the presence of the strong hyperfine coupling between the electron spin and the nitrogen nucleus. In effect, the electron "sees" the field of the nitrogen nucleus perturbed by the Earth's magnetic field rather than the Earth's magnetic field perturbed by the nitrogen nucleus and so the thermal polarization of the electron spins, and in turn the maximum possible DNP enhancements, are much greater than is predicted by the electron Zeeman interaction in the external magnetic field alone.

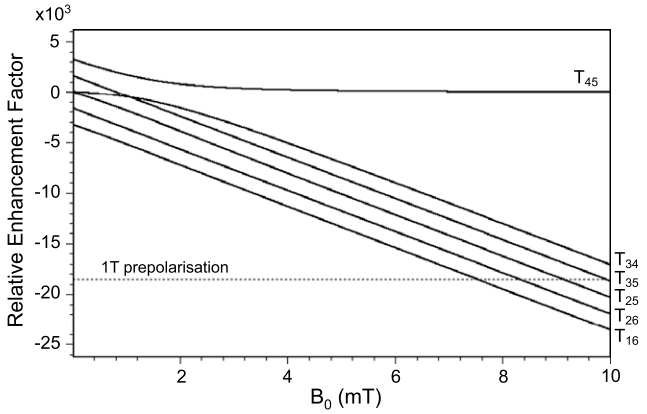

Fig. 4. Maximum DNP enhancement factors relative to thermal polarization in the Earth's magnetic field for the transitions: T_{16}, T_{26}, T_{25}, T_{35}, T_{34} and T_{45} over a range of polarizing fields from the Earth's field to 10 mT. The horizontal line indicates the maximum enhancement factor, relative to thermal equilibrium in the Earth's field, achievable using a 1 T prepolarization magnet. In this calculation, $A = 45$ MHz, $s = 1$, $f = 1$ and $\rho = 0.5$.

3. Results and discussion

Fig. 5 presents a comparison of Earth's field NMR spectra acquired of 100 mL of water doped with 1.5 mM of TEMPO. The spectrum in gray was acquired with an 18.7 mT prepolarizing field generated by an electromagnet. The spectrum in black was acquired with a DNP irradiation at 68 MHz and no prepolarization. By integrating the peaks it is found that the DNP signal enhancement is greater than the prepolarization signal enhancement by a factor of −6.5. Extrapolating this back to the Earth's field strength of 54 μT, this is an enhancement over thermal equilibrium polari-

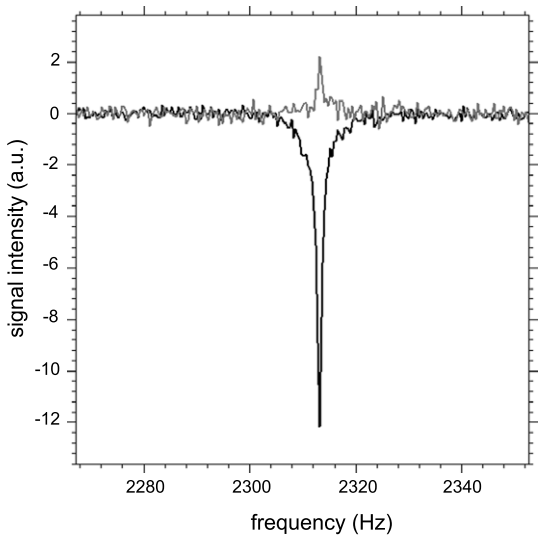

Fig. 5. Earth's field NMR spectra of 100 mL of water doped with 1.5 mM of TEMPO using 18.7 mT prepolarization (gray) and 68 MHz DNP irradiation in the Earth's field (black). The DNP enhancement is −6.5 times larger than the prepolarization enhancement, which is equivalent to a DNP enhancement factor of −2250 over thermal equilibrium polarization at 54 μT.

zation of −2250. A larger signal enhancement of approximately −3100 over thermal equilibrium can be achieved with a DNP irradiation at 131.5 MHz in the presence of a 2.7 mT prepolarizing field. This is illustrated by the inset of Fig. 3, a field cycled DNP experiment which shows that the T_{16} resonance provides the largest signal enhancement under these experimental conditions.

While the signal enhancements demonstrated in the inset of Fig. 3 are larger than that in the Earth's field alone, this experiment is not optimized because full saturation of the transitions has not been achieved. This is due in large part to the inhomogeneity of the polarizing coil relative to the size of the sample. This inhomogeneity broadens the EPR spectral lines to such an extent that, with an RF source of 50 W, only partial saturation was possible. However, even with this hardware limitation, an SNR advantage of almost an order of magnitude is observed when comparing the field cycled DNP approach to prepolarization by an electromagnet at 18.7 mT.

Fig. 6a presents a 2D ^{19}F–^{1}H COSY acquired of neat 2,2,2-trifluoroethanol in the Earth's magnetic field using the pulse sequence in Fig. 1, which includes DNP irradiation at 131.5 MHz in the presence of a prepolarization field of 2.5 mT. The 100 mL sample was doped with 1.5 mM TEMPO. The spectrum was acquired in approximately 11 h with four signal averages. Fig. 6b presents a simulated COSY spectrum for comparison. The experimental spectrum displays significantly superior SNR and resolution compared to the previously reported 2D Earth's field NMR spectra [9] and was achieved using a much smaller sample size. In addition the ULF noise interference is greatly reduced through the use of a Faraday screen.

Comparison of the experimental and simulated COSY results highlights some of the interesting spectroscopic features of the DNP experiment. Fig. 7a presents a 1D projection, taken along the f_1 dimension, of the experimental 2D COSY spectrum in Fig. 6a. Fig. 7b presents a 1D simulated spectrum for comparison. These 1D spectra illustrate a few of the interesting features of DNP enhanced Earth's field NMR spectroscopy. First it is clear that the central proton peak, which corresponds to the OH group, is only weakly enhanced in the DNP spectrum. The OH proton is in rapid exchange and a comparison of these spectra reveals that it does not couple as strongly as the other protons to the unpaired electron spins. Second, it is clear that the remaining quartet of proton peaks are enhanced to a much greater degree than the fluorine peaks. This suggests that the coupling of these protons to the electrons is much more efficient than the coupling of the fluorine spins to the unpaired electrons. The third point of interest is the suggestion of high-resolution structure which is observed in the simulated spectrum due to the fact that the hetero-nuclear J coupling constant between the ^{1}H and ^{19}F nuclei (∼8.5 Hz) falls into the strong coupling regime when compared to the difference in Larmor frequency of the ^{1}H and ^{19}F nuclei (135 Hz). A vector model to describe ultra-low field NMR spectra in this strong coupling regime has been presented by Appelt et al. in [28]. Under this theory, 12 high-resolution lines would be expected for the ^{19}F spectrum and 16 high-resolution lines plus one uncoupled line would be expected for the ^{1}H spectrum. An improvement in resolution of the experimental setup, either through improved shimming and/or a decrease in the free radical concentration will potentially reveal more experimental information about this high-resolution structure.

4. Conclusion

In this work, it has been shown that dynamic nuclear polarization provides a very powerful mechanism for polarization enhancement of multi-dimensional Earth's field NMR spectroscopy. A theoretical analysis indicates that large polarization enhancement factors are possible using DNP with nitroxide free radicals where the unpaired electron spins experience a strong hyperfine coupling to a neighboring ^{14}N nucleus. Comparing this DNP approach to the more traditional signal enhancement idea of prepolarization, the sensitivity enhancement factors which can be achieved using field-cycled DNP with an irradiation frequency in the range of 100–150 MHz are on the same order of magnitude as that achieved using a 1 T prepolarizing field and no DNP.

Experimental results show that DNP enhanced Earth's field NMR can be implemented either in the Earth's magnetic field or in a weak prepolarizing field to achieve enhancements of 2000–3000, almost an order of magnitude better than the enhancements achieved using an 18.7 mT electromagnet for prepolarization.

DNP enhanced Earth's field NMR was successfully used to acquire a high-quality 2D ^{19}F–^{1}H COSY spectrum of 2,2,2-trifluoroethanol. Comparison with simulation indicates that the DNP approach provides additional information about the sample through the coupling factors which determine the observed signal enhancement.

Future work includes the optimization of the system such that the maximum DNP enhancement can be observed. It is anticipated that this will require a more uniform prepolarization electromagnet for the field-cycle DNP approach as well as a more complete understanding of the combined effects of saturation and coupling factor at ultra-low fields, similar to that presented for the high field case in [27]. With respect to the goal of high SNR, high-resolution multi-dimensional Earth's field spectroscopy, a compromise needs to be reached between leakage factor, f, and by extension DNP enhancement factor, and homogeneous line broadening such that high SNR multi-dimensional spectra with a resolution on the order of 0.1 Hz can be achieved. It is also anticipated that this method will be highly advantageous for looking at other nuclei besides ^{19}F and ^{1}H.

Experimental issues such as sample heating due to power deposition by B_{1RF} irradiation must also be further examined and understood in order to optimize this methodology.

5. Experimental

A photo of the entire experimental apparatus is presented in Fig. 8. All experiments were performed indoors using a Terranova

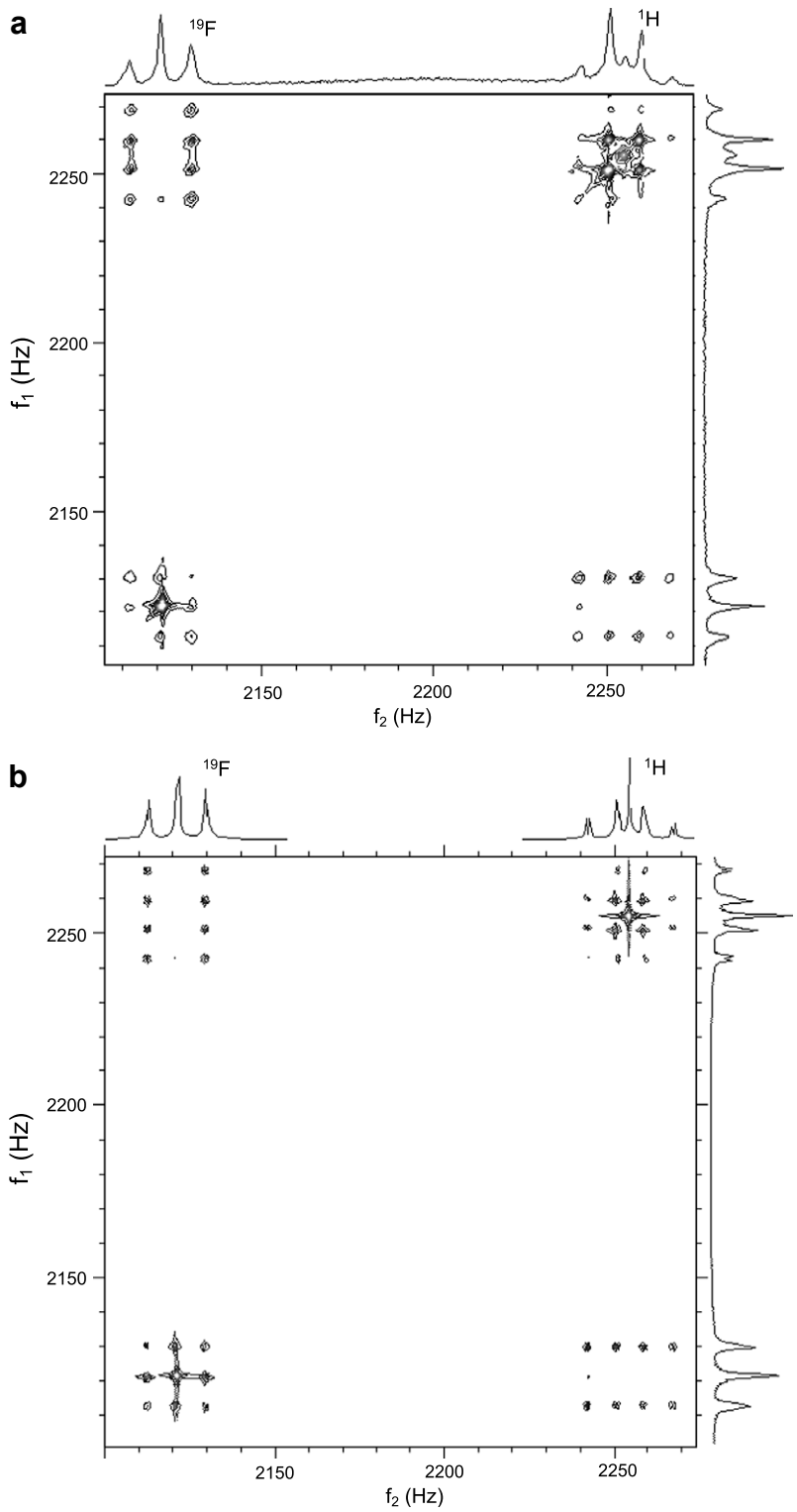

Fig. 6. (a) 2D ^{19}F–^{1}H COSY of 2,2,2-trifluoroethanol doped with 1.5 mM TEMPO acquired in the Earth's field with DNP irradiation at 131.5 MHz in a prepolarization field of 2.5 mT. A reference scan was acquired between each t_1 step to track and offset any fluctuations in the Earth's magnetic field. The experiment took 11 h to complete and was acquired with four signal averages. (b) A simulated 2D ^{19}F–^{1}H COSY spectrum corresponding to the experimental spectrum in (a).

MRI Earth's field system (Magritek, Wellington, New Zealand). This system is equipped with a 3.13 mT/A electromagnet for prepolarization as well as three orthogonal gradients used for first order shimming. A 10 mm thick copper box was used as a Faraday shield. Due to the use of this shield, a delay of 350 ms is typically introduced between the switch off of the polarizing coil and the excitation pulse to allow for the decay of any induced eddy currents. This delay was shortened to 150 ms for the COSY experiment with DNP because a smaller prepolarization field was used. Two homebuilt low-pass birdcage coils were used for the RF excitation. Both coils were 100 mm long, 58 mm in diameter and were designed using BirdcageBuilder version 1.0 (Penn State, PA, USA). The RF irradia-

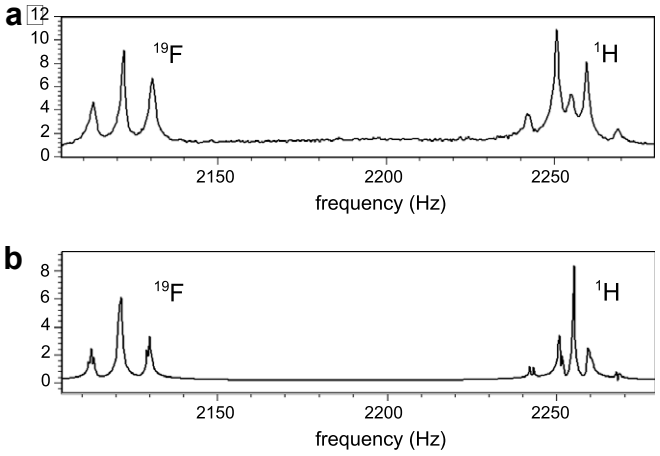

Fig. 7. (a) A 1D projection along f_1 of the 2D COSY spectrum in Fig. 7(a). (b) A simulated 1D NMR spectrum of 2,2,2-trifluoroethanol for comparison with (a). Note the relatively weak enhancement of the central ^{1}H peak in the experimental spectrum, which indicates that the proton associated with the OH group is not as strongly coupled to the unpaired electron spins as the other protons. The other proton peaks, associated with the CH_2 group, are more strongly enhanced than the ^{19}F peaks, indicating that the coupling between these protons and the electron spins is greater than that between the ^{19}F nuclei and the electron spins.

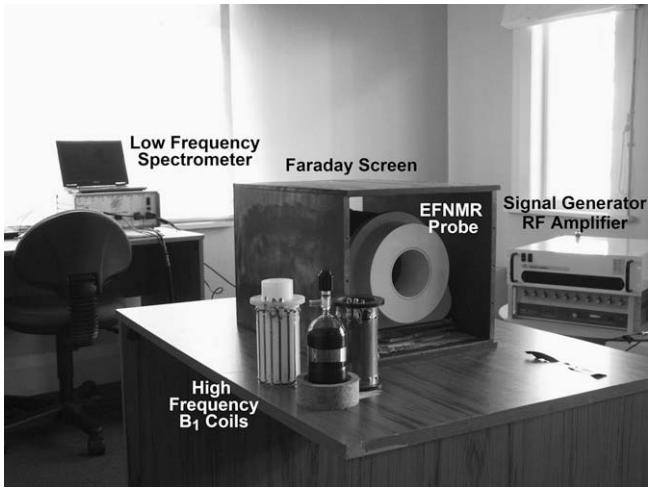

Fig. 8. A photo of the Earth's field NMR setup which consists of a Magritek Terranova MRI Earth's field system, a 10 mm thick copper Faraday screen, a PTS RF synthesizer, a Tomco high powered amplifier and two homebuilt birdcage coils for RF irradiation at 68 MHz and 131.5 MHz, respectively.

tion was generated by a PTS synthesizer (Programmed Test Sources, Littleton, MA, USA) and amplified by a Tomco AlphaSA high powered amplifier (Tomco, Norwood, SA, Australia). All simulations and data processing were performed using the Prospa software package (Magritek, Wellington, New Zealand).

The samples used were water and neat 2,2,2-trifluoroethanol (Sigma–Aldrich, USA), each doped with 1.5 mM 2,2,6,6-tetramethylpiperidine 1-oxyl (TEMPO) (Sigma–Aldrich, USA). Both samples were deoxygenated to increase T_1 and the leakage factor, f. The leakage factor for the doped water sample was 0.82 and T_1 was measured to be 1.1 s. Due to the limited signal available for the trifluoroethanol sample without the use of DNP, the leakage factor for this sample could not be measured accurately. It was estimated to be approximately 0.7 with a T_1 of 1 s.

It is known that there exists a temporal drift in the Earth's magnetic field [29]. This drift can result in a Larmor frequency drift of several Hz over a period of hours or even minutes. In order to prevent this drift from degrading the resolution of the long 2D COSY measurement, reference scans were acquired between each t_1 step. These reference scans were used to monitor any changes in the Larmor frequency of the sample and any observed changes were opposed by adjusting the current in a B_0 lock coil incorporated into the gradient set within the EFNMR probe. Using this method, the observed Larmor frequency can be effectively stabilized over many hours to within the linewidth of the reference signal.

Acknowledgments

The authors thank Mark Hunter, Ben Parkinson and Robin Dykstra for help with the experimental setup, Guillaume Madelin for help with the theoretical analysis, Craig Eccles for software support and Andrew Coy for useful discussions. The authors gratefully acknowledge the New Zealand Foundation for Research Science and Technology for financial support.

References

[1] M. Packard, R. Varian, Phys. Rev. 93 (1954) 941.
[2] G.J. Béné, Phys. Rep. 58 (1980) 213–267.
[3] J. Stepisnik, V. Erzen, M. Kox, Magn. Reson. Med. 15 (1990) 386–391.
[4] A. Mohoric, J. Stepisnik, M. Kos, G. Planinsic, J. Magn. Reson. 136 (1999) 22–26.
[5] M.E. Halse, A. Coy, R. Dykstra, C. Eccles, M.W. Hunter, R. Ward, P.T. Callaghan, J. Magn. Reson. 182 (2006) 75–83.
[6] S. Appelt, F.W. Häsing, H. Kühn, J. Perlo, B. Blümich, Phys. Rev. Lett. 94 (2005) 197602.
[7] S. Appelt, H. Kühn, F.W. Häsing, B. Blümich, Nat. Phys. 2 (2006) 105–109.
[8] S. Appelt, F.W. Häsing, S. Baer-Lang, N.J. Shah, B. Blümich, Chem. Phys. Lett. 348 (2001) 263–269.
[9] J.N. Robinson, A. Coy, R. Dykstra, C.D. Eccles, M.W. Hunter, P.T. Callaghan, J. Magn. Reson. 182 (2006) 343–347.
[10] P.T. Callaghan, C.D. Eccles, J.D. Seymour, Rev. Sci. Instrum. 68 (1997) 4263–4270.
[11] P.T. Callaghan, C.D. Eccles, T.G. Haskell, P.J. Langhorne, J.D. Seymour, J. Magn. Reson. 133 (1998) 148–154.
[12] P.T. Callaghan, R. Dykstra, C.D. Eccles, T.G. Haskell, J.D. Seymour, Cold Reg. Sci. Technol. 29 (1999) 153–171.
[13] O.R. Mercier, M.W. Hunter, P.T. Callaghan, Cold Reg. Sci. Technol. 42 (2005) 96–105.
[14] I.M. Savukov, Phys. Rev. Lett. 94 (2005) 123001.
[15] R. McDermott, A.H. Trabesinger, M. Muck, E.L. Hahn, A. Pines, J. Clarke, Science 295 (2002) 2247–2249.
[16] A. Abragam, Phys. Rev. 98 (1955) 1729.
[17] N. Kernevez, H. Glenat, IEEE Trans. Magn. 27 (1991) 5402.
[18] I. Solomon, Phys. Rev. 99 (1955) 559.
[19] T. Guiberteau, D. Grucker, J. Magn. Reson. B 110 (1996) 54–77.
[20] I.I. Breit Rabi, Phys. Rev. 38 (1931) 2082.
[21] K. Lang, M. Moussavi, E. Belorizky, J. Phys. Chem. A 101 (1997) 1662–1671.
[22] G. Planinsic, T. Guiberteau, D. Grucker, J. Magn. Reson. Ser. B 110 (1996) 205–209.
[23] C. Polyon, D.J. Lurie, W. Youngdee, C. Thomas, I. Thomas, J. Phys. D 40 (2007) 5527–5532.
[24] T. Guiberteau, D. Grucker, J. Magn. Reson. Ser. A 105 (1993) 98.
[25] D.J. Lurie, I. Nicholson, J.R. Mallard, J. Magn. Reson. 95 (1991) 405–409.
[26] D.J. Lurie, Appl. Magn. Reson. 3 (1992) 917.
[27] B.D. Armstrong, S. Han, J. Chem. Phys. 127 (2007) 104508.
[28] S. Appelt, F.W. Häsing, H. Kühn, B. Blümich, Phys. Rev. A 76 (2007) 023420.
[29] R.T. Merrill, M.W. McElhinny, P.L. McFadden, The Magnetic Field of the Earth: Paleomagnetism the Core and the Deep Mantle, Academic Press, San Diego, 1998.